Heliyon 10 (2024) e33443

Contents lists available at ScienceDirect

Heliyon

journal homepage: www.cell.com/heliyon

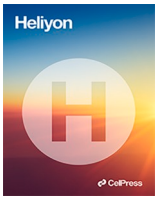

Research article

Tailoring structural and optical properties of ZnO system through elemental Mn Doping through First-principles calculations

Rasool Akhtar Alias Osama [a,d,*], Sadia Abdul Samad [a], Samia Saher [b], Muhammad Rafique [c], Rebecca Cheung [a]

[a] Institute for Integrated Micro and Nano Systems, IMNS School of Engineering, University of Edinburgh, UK
[b] GCU, Government College University, Pakistan
[c] HIT, Harbin Institute of Technology, PR China
[d] Mehran University of Engineering & Technology, S.ZAB Campus Khairpur Mir's, Pakistan

ARTICLE INFO

Keywords:
Doped ZnO
Band structure
Optics
Computational study
Phonon Dispersion
Temperature Profile

ABSTRACT

In this study, band structure and optical properties of Manganese (Mn) doped ZnO are investigated adopting first-principles study calculations. It is observed that, by addition of Mn in ZnO crystal, the electrical properties like conductivity and dielectric function of material have been improved. The elastic constants for the elements are also calculated which shows that the element is stable after addition of dopant. The computational study is done on CASTEP and Material Studio. The ZnO system is simulated and atoms of Mn has been added replacing Zn atoms. The properties that studied are band structure and optics including conductivity, reflectivity, dielectric function, absorption and refractive index. Furthermore, this study also includes calculation of Elastic constants, XRD Spectra, Phonon dispersion and Temperature profile of doped ZnO systems. The computational study produced promising results and experimental approach can be adopted to reinforce the outcomes of this study.

1. Introduction

The primary source of energy has been the fossil fuels for decades. But such resources have become scarce and also cause environmental pollution, which has diverted the attention of researchers towards renewable and self-sustained energy resources [1–4]. In addition the advent of electronics to control electrical power has emerged as a need of low power and self-powered systems. So, there are several approaches used to utilize the eco-friendly, self-powered and energy conservative options [5,6].

Among the options, one of the prominent source of energy is mechanical energy, which is freely available and can be converted to electrical energy using piezoelectric sensors. These sensors are made of different materials which are Aluminium Nitrate, Cadmium Sulphide, Zinc Sulphide and Zinc Oxide, etc [6–8].

ZnO semiconductor is one of the emerging material to be used in solar cells, photocatalytic degradation, gas sensors and piezoelectric sensors [1,9]. Compared to other semiconductors, ZnO has better photoelectric properties, high gas sensitivity, non-toxicity and it is chemically stable, exhibiting high binding energy so can be used extensively in optoelectronic applications [10].

However, owing to the larger band gap, it has limited application in the visible range of light [11]. Due to larger band gap, electrons

* Corresponding author. Institute for Integrated Micro and Nano Systems, IMNS School of Engineering, University of Edinburgh, UK.
E-mail addresses: rasool.akhtar@ed.ac.uk (R.A. Alias Osama), s2440592@ed.ac.uk (S.A. Samad), samiasaher1@gmail.com (S. Saher), rafique@hit.edu.cn (M. Rafique), R.Cheung@ed.ac.uk (R. Cheung).

https://doi.org/10.1016/j.heliyon.2024.e33443
Received 24 February 2024; Received in revised form 19 June 2024; Accepted 21 June 2024
Available online 22 June 2024

easily combine with holes and reduces the performance of the material [12].

Few applications of ZnO doped systems include photo degradation and energy storage [13,14]. In literature ZnO has been used in environmental application of photocatalytic degradation of pollutants [13,15]. Excitation of ZnO generates electron in conduction band and holes in valence bands which undergoes chemical reactions and form by-products like H_2O and CO_2 [13]. The study reveal that the doping of ZnO with transition metal enhanced the dielectric property and electrical conductivity of the system which is viable for energy storage application [14].

ZnO structure has a unique feature of having empty octahedral sites, which are viable for incorporating dopants in it. ZnO itself is an n-type semiconductor but a number of attempts have been made to modify it to a p-type semiconductor. ZnO electrons has higher mobility than other semiconductors which leads to the better quantum efficiency [16–19].

The choice of dopants depends on the number of factors that are taken into consideration [20]. The factors are modeling energy, ionic radius, resistivity, and transmittance [20]. The dopant should have low modeling energy so that the electrostatic force can be created between the clusters of atoms [12,20]. The ionic radius of the atoms should be low so that it may not distort the lattice of crystal [21]. The conductivity of the material should increase which may aid to the mobility of the electrons [12,22]. Also the transmittance of the material should be evident from lower reflectivity and absorption [21]. It should increase the transmittance at shorter wavelength. Dopants must have good solubility [22,23].

In recent times, it has been shown that the properties of ZnO has improved by doping with transition elements [11,12,24]. The band gap of ZnO decreases with the addition of such dopant [11,12]. There is a lot of literature available and research is being done on the evolution of ZnO in such particular applications.

The choice of transition metals as dopants has significantly gained importance as they possess superior characteristics [1,24,25]. The studies has proved that the addition of Manganese in ZnO system has comprehensively improved the properties and performance of ZnO due to its electronic configuration and magnetic effect [26]. It is found to be the optimum choice for researchers among all the transition metals [26].

Although plenty of research is done on the study of introducing transition element in ZnO system but addition of Mn is yet to be studied comprehensively separately. This study is focused on the doping of Mn in ZnO system and its computational evaluation of the characteristics.

These studies suggest that, the doping can improve the performance and the impurities can be added atom to atom. However, another way to add the atom is to add percentage impurity in the atom individually. It can significantly modify the electronic, magnetic and optical properties of recommended material [18,19,26,27].

2. Computational details and geometry models

CASTEP (version 22.11) has been used to investigate the electronic structure and optical properties of Transition metal (Manganese) doped ZnO utilizing Generalized Gradient Approximation (GGA) method [20,26]. ZnO supercell $2 \times 2 \times 2$ and the calculations were performed with plane-wave basis set having ultasoft pseudopotentials with cut-off energy of 450 eV. Calculations done are spin polarized. The $4 \times 4 \times 4$ thick k-point mesh is used. Geometry optimization is carried out till the Hellmann-Feynman forces reach 0.01 eV/Å value and total energy change less than 10^{-6} is calculated. The calculations are done with and without impurities in accordance with the literature [1,4,6–12,18–37].

Although, in previous studies [26,38,39] it is suggested that the semi-local PBE functionals underestimates the band gap and so can effect the electronic properties. Therefore, a simple solution to this problem is to use hybrid functionals, which has been demonstrated for the monolayer graphene, boron and nitrogen doped graphene structures [40–42]. In addition to it, due to disputed difference between GGA-PBA and hybrid functional predictions, we computed both functional to determine band gap. Both computational parameters revealed almost similar band gap values with a minimal variation of approx. 0.01–0.03 eV in the band gap results.

First, a pure ZnO supercell is modelled, then 2 Zn atoms are replaced by Mn atoms to form a doped supercell. The doping percentage can be calculated as 14.2 %. Similarly, in the next step 4, Mn atoms are added to observe the changes in parameters after increase of dopants. The doping percentage can be calculated as 28.4 %.

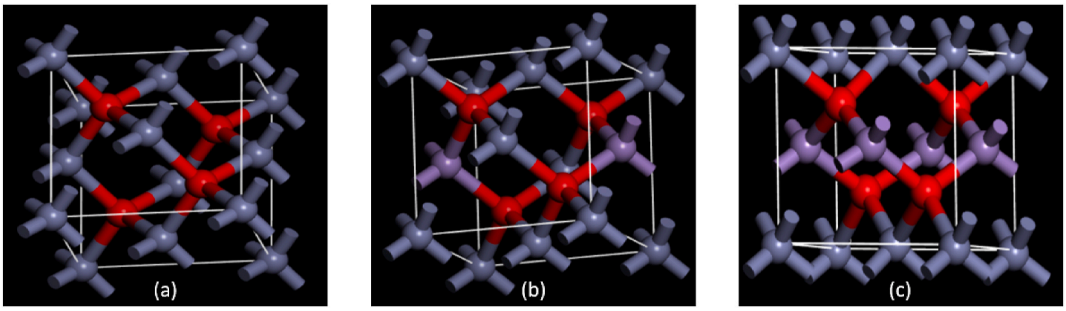

Fig. 1. (a) Atomic structures of 3D view of optimized geometry of ZnO supercell (Red colour indicates Oxygen atoms, Grey indicates Zn atoms and Purple indicates Mn atoms). **(b)** Atomic structures of 3D view of optimized geometry of 2Mn doped ZnO supercell. **(c)** Atomic structures of 3D view of optimized geometry of 4Mn doped ZnO supercell.

3D views of the typically relaxed structure model of Pure ZnO system is illustrated in Fig. 1(a). Similar structure model of 2Mn and 4Mn doped ZnO system is illustrated in Fig. 1(b) and (c).

3. Results and discussions

3.1. Band structure, density of states and magnetic effect of Mn doped ZnO

In this study, band structure and DOS of pure ZnO along with two different doping levels of Mn have been investigated. To obtain the band structure and DOS, designed geometries are fully optimized and atoms are allowed to relax [16,19,20,27,43]. The relaxed geometries of elements reveal significant variation in the bond lengths between the atoms. The bond lengths of pure Zn–O varies from 2.005 Å to 2.001 Å. Similarly, the bond lengths of Mn–O varies from 2.005 Å to average of 2.040–1.894 Å.

Band structure is obtained on G-F-Q-Z path. A 4 × 4 × 4 K-grid is employed to get density of states. Total DOS is calculated for all systems. Computed band structure of pure ZnO reveals a wide band gap of 0.603 eV as shown in Fig. 2(a).

After the addition of donor atoms i.e. 2 Mn atoms, the band structure overlaps which means the material has become more conductive and now a small excitation can drive the electrons to flow as shown in Fig. 2(b).

Similarly further 2 Mn atoms has been added to the crystal structure which make it a total of 4 Mn atoms and more overlapping is obtained in the results as shown in Fig. 2(c).

Fig. 3 shows the DOS of all the three designed systems. It is clear that in pure ZnO system has the greater concentration of electrons near fermi level, which is in valence band. After addition of 2 Mn atoms in the ZnO system the concentration of electron has shifted to conduction band.

Similarly, the DOS of 4 Mn doped ZnO also suggests that overall concentration has become closer to the fermi level and can help the electrons mobilize easily.

In a nutshell, it can be said that the addition of Mn in ZnO system can make it conductive as clearly visible in the figures. It can also be a basis set for the experimental study.

It is also important to discuss the spin contamination problem. As it is known that the spin contamination occus mostly in unrestricted Hartree-Fock (UHF) and unrestricted Møller-Plesset calculations. However, in DFT calculations spin contamination problem does not occur so often, even when unrestricted Kohn-Sham orbitals are being used. CASTEP/Material Studio program does not provide direct solution for spin contamination, the partial occupancies of the Bloch states can be investigated within minimization of the total energy [16,19,27,41–44]. In previous studies, Mn doped compounds have exhibited the properties of high spin polarization, low saturation magnetization and low mangetic damping constants [24,37,45–47]. Also the compound exhibit strong spin-orbit coupling when more Mn atoms added to it [48,49].

3.2. Optical properties

Previously, optical parameters of pure ZnO and Mn doped has been studied [9,11,12,20,35], similarly in this research optical parameters including conductivity, refractive index, reflectivity, absorption and dielectric function have been studied. The approximations used are the same as earlier research which are found to be reliable and accurate [9,11,19,20,35]. PBA approximation has been taken into account for analysis of the properties through DFT.

Pure and Mn doped ZnO system's refractive index (n) has been obtained and a comparative graph is shown in Fig. 4. The refractive index value at 0 eV is termed as static and for pure ZnO system displays 2.2 peak. But after the addition of dopants the static has been raised to almost 6 after addition of 2Mn atoms in the system. And to 8 after addition of 4Mn atoms in the system, which is evident from Fig. 4. The peaks obtained depend on the number of Mn atoms added in the system. It can be seen that the Mn addition only changed the static refractive index and at higher energy range the variation is very minute.

Pure and Mn doped ZnO system's absorption coefficients (α) obtained and a comparative graph is shown in Fig. 5. It can be observed from the plot that the principal peak is at 15 eV around 325000 cm^{-1} pure ZnO system. After the addition of Mn, the system's

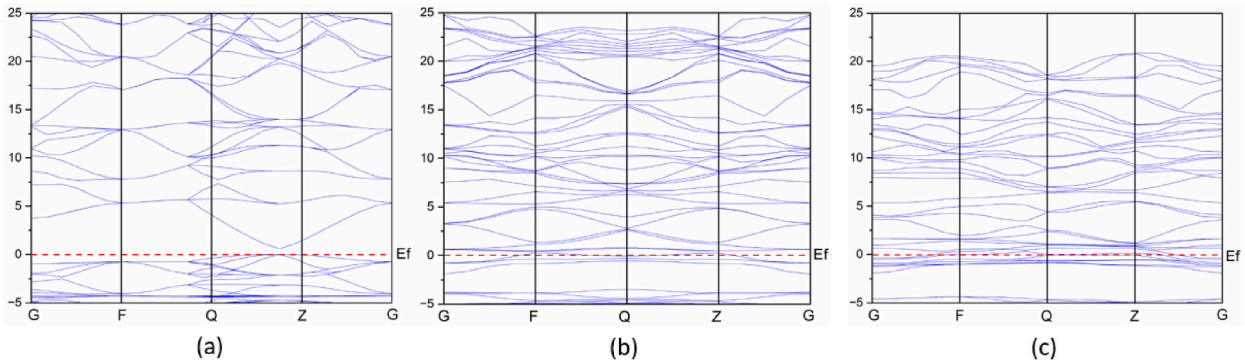

Fig. 2. Band structure of **(a)** pure ZnO, **(b)** 2Mn doped ZnO system & **(c)** 4Mn doped ZnO system.

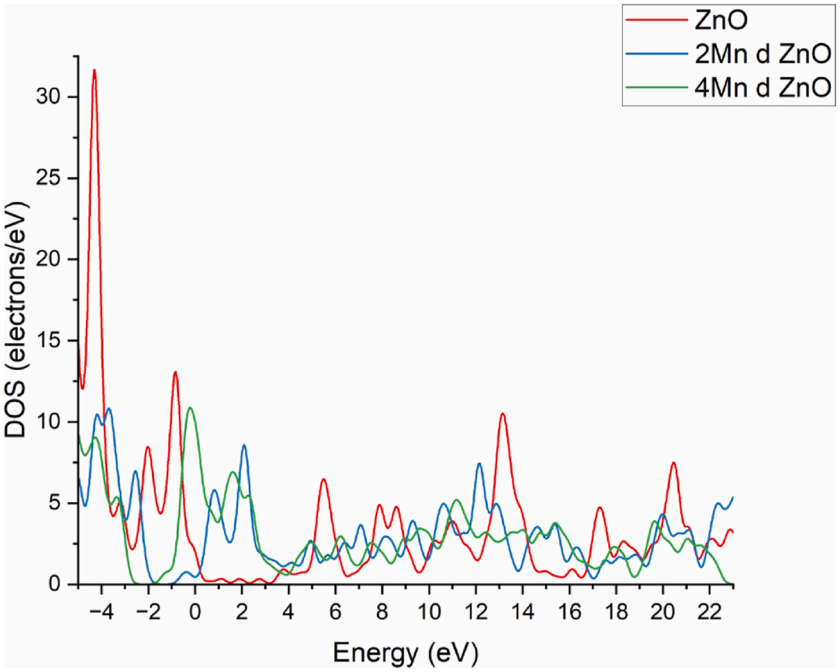

Fig. 3. Comparison of DOS of ZnO & doped ZnO systems.

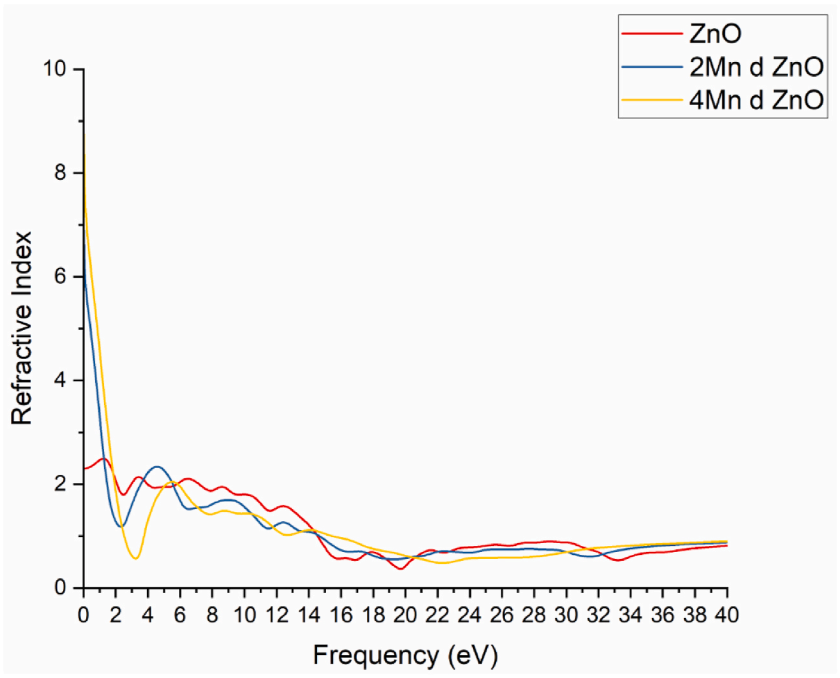

Fig. 4. Comparison of Refractive Index of ZnO & doped ZnO systems.

coefficient has been observed to increase at lower ranges of eV which is an evidence of red shift. Also the principal peaks have changed which is evident that the variation has been made in inter and intra band transitions. The highest peak 250000 cm^{-1} after incorporation of 2Mn atoms is observed at 16.5 eV as shown in Fig. 5. And the highest peak of 230000 cm^{-1} can be observed at around 18eV by addition of 4Mn atoms.

Pure and doped ZnO systems' reflectivity is also illustrated in Fig. 6. It can be seen clearly that the static reflectivity is improved after the addition of Mn atoms as dopants in the system. New static values obtained are 0.53 and 0.60 for 2Mn doped and 4Mn doped

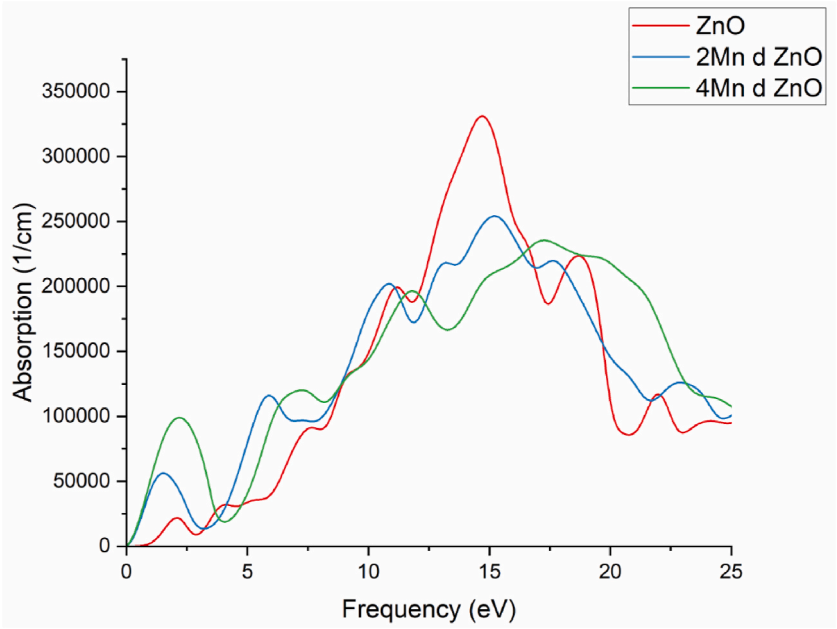

Fig. 5. Comparison of Absorption Coefficient of ZnO & doped ZnO systems.

ZnO system respectively. At higher energy ranges, the change is not significant and at last the values become almost equal after some fluctuations. Also it can be concluded that higher reflectivity values at lower energy ranges is evidence of red shift.

The conductivity of pure and doped ZnO system is illustrated in Fig. 7. The conductivity has been significantly increased after the addition of Mn atoms in the system. The peak values of 2.2 and 3.9 can be seen in lower energy ranges which is evidence of red shift. Also, the higher peak values of pure ZnO system can be seen at higher energy ranges. It can be concluded that at lower energy ranges, doped ZnO system has more conductivity than pure ZnO system while at higher energy ranges, pure ZnO system has higher conductivity than the doped ZnO system.

The dielectric function of pure and doped ZnO system is also shown in Fig. 8. The static value of dielectric function is vital for

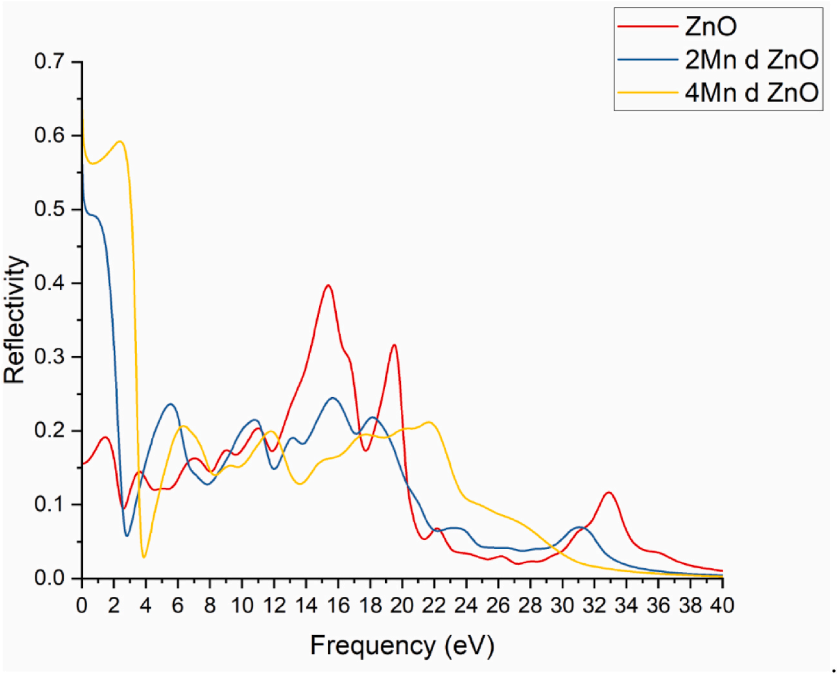

Fig. 6. Comparison of Reflectivity of ZnO & doped ZnO systems.

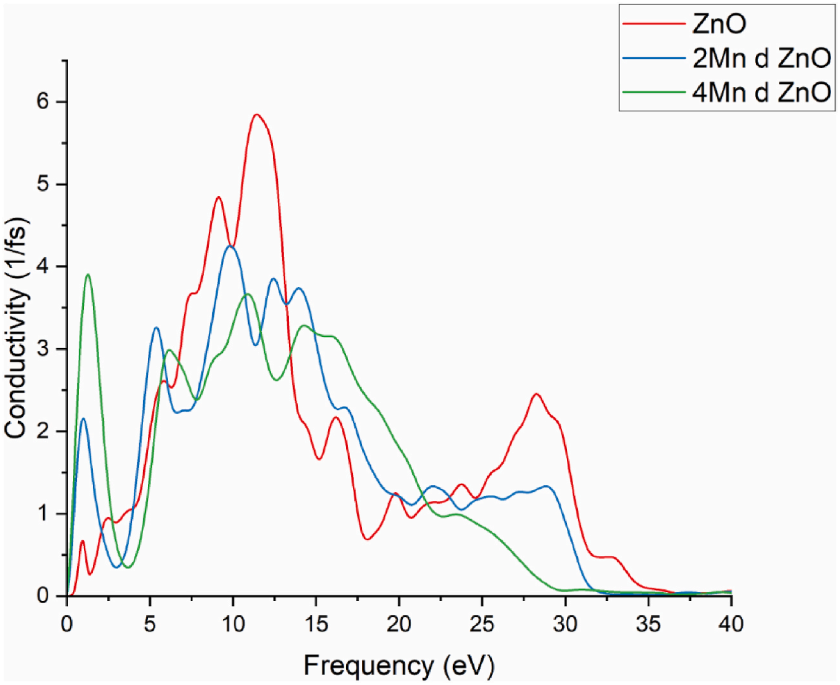

Fig. 7. Comparison of Conductivity of ZnO & doped ZnO systems.

observing the variation in behavior of the system after addition of dopants. The static dielectric function for pure system is computed as 6 which has been increased to values of 40 and 60 for the 2Mn and 4Mn doped systems respectively.

Optical properties of pure and doped ZnO systems are evidence of the fact that the addition of Mn atom has improved the properties of the system.

3.3. Elastic constants

The elastic constants (C_{11}, C_{12} and C_{44}) were calculated using the CASTEP and were found to be satisfying the condition of stability for a cubic structure crystal, the conditions are:

$C_{11}–C_{12} > 0$

$C_{11} + 2C_{12} > 0$

$C_{44} > 0$

The computed constants are given in the following Table 1.

The constants exhibit that the structures formed are satisfying the conditions of stability and modified geometry is elastically stable. Also it is evident that the added Mn atoms have been accepted by the lattice [35].

3.4. X-ray power diffraction (XRD) spectra

The XRD Spectra of the simulated systems have been computed using Powder Diffraction function of Reflex module of Material Studio. The standard card for pure ZnO is JCPDS card number 36–1451. Fig. 9 shows that no new phases are introduced only the peaks are broadened with slight shift in 2-Theta. The intensity of peaks also decreases as the dopants are added. The atomic radii of Zn and Mn has been computed to be 161 p.m. and 142 p.m. respectively. The difference of atomic radii creates strain in the atomic lattice and the slight variation in angle has been observed in occurrence of peaks [9,16,17,22,50,51]. It means the dopant has been accepted by the lattice structure and can be used for more applications [6,8,31].

3.5. Phonon dispersion

The Phonon dispersion of the doped system has been analyzed to evaluate the dynamic stability of the system. 2Mn doped system phonon dispersion is in Fig. 10 (a), which reveals that there is only one soft band or imaginary mode below the zero frequency, which usually appears for the metals and this configuration can be termed as dynamically stable. In the next configuration, few modes have appeared below the zero frequency for 4Mn doped system as shown in Fig. 10(b). It seems less stable than the first configuration but

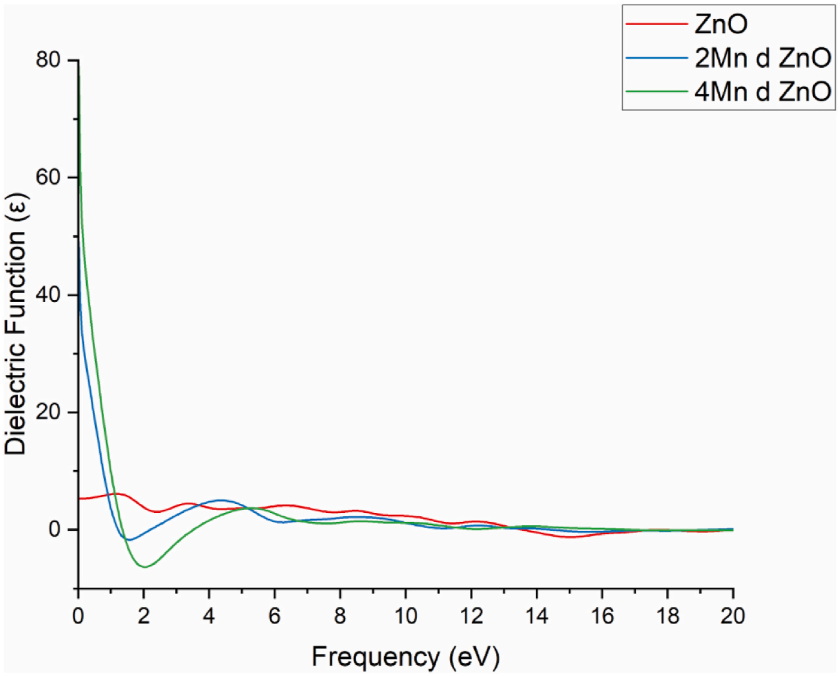

Fig. 8. Comparison of Dielectric Function of ZnO & doped ZnO systems.

Table 1
Elastic Constants of pure and doped ZnO systems.

Element	Elastic Constants		
	C_{11}	C_{12}	C_{44}
ZnO	188.52	109.00	56.06
2Mn doped ZnO	200.36	118.01	37.29
4Mn doped ZnO	221.12	129.51	23.53

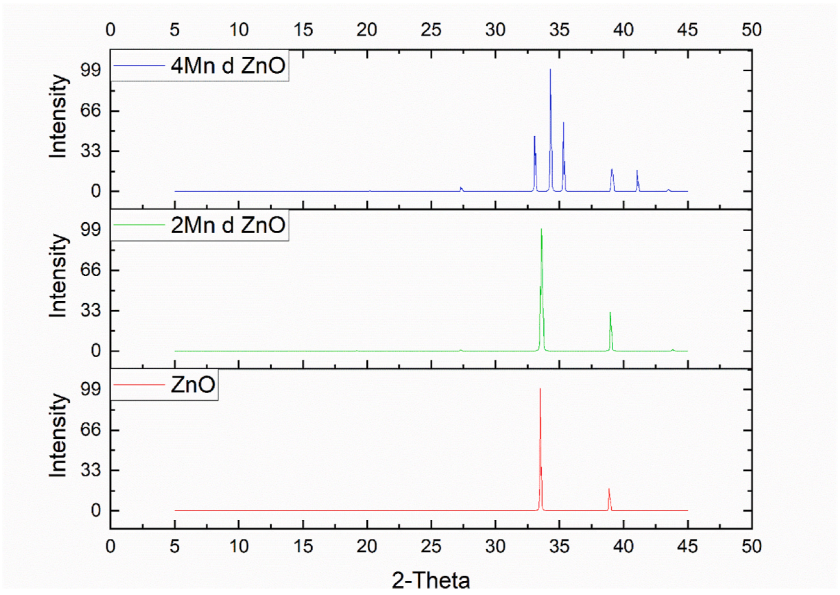

Fig. 9. Comparison of XRD Spectra of ZnO & doped ZnO systems.

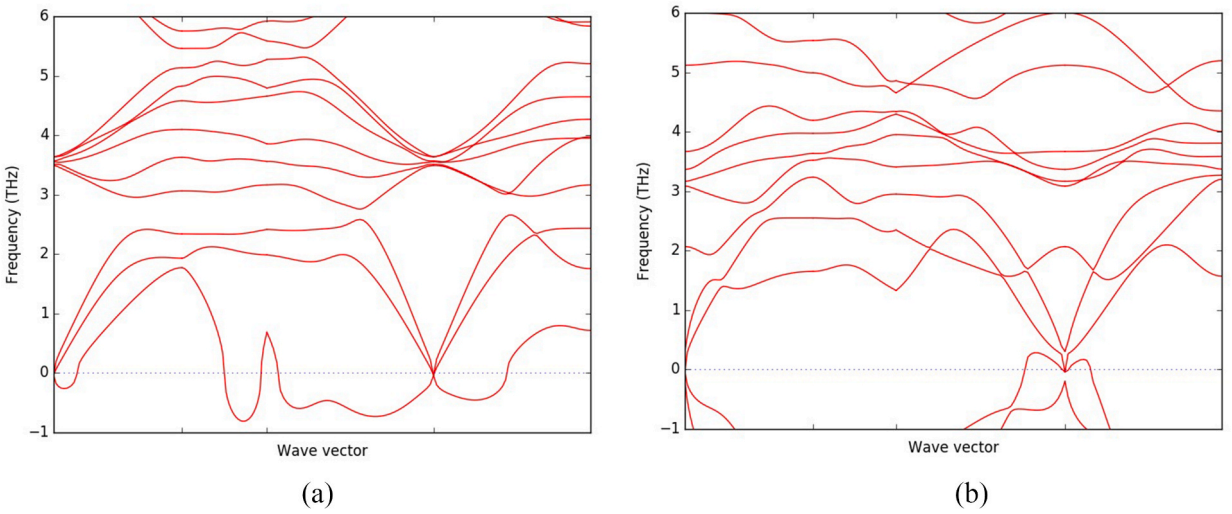

Fig. 10. Phonon Dispersion of **(a)** 2Mn doped ZnO system & **(b)** 4Mn doped ZnO system.

still it can be counted as dynamically stable as the concentration of soft band is less. These soft modes are marginal and may appear in the phonon dispersion of metals.

3.6. Thermal stability

The molecular dynamic calculation of designed configuration was performed using NVT ensemble at 900 K. The temperature profile is shown in Fig. 11. It indicates that the variation in response to temperature is not prolonged for both configurations and they

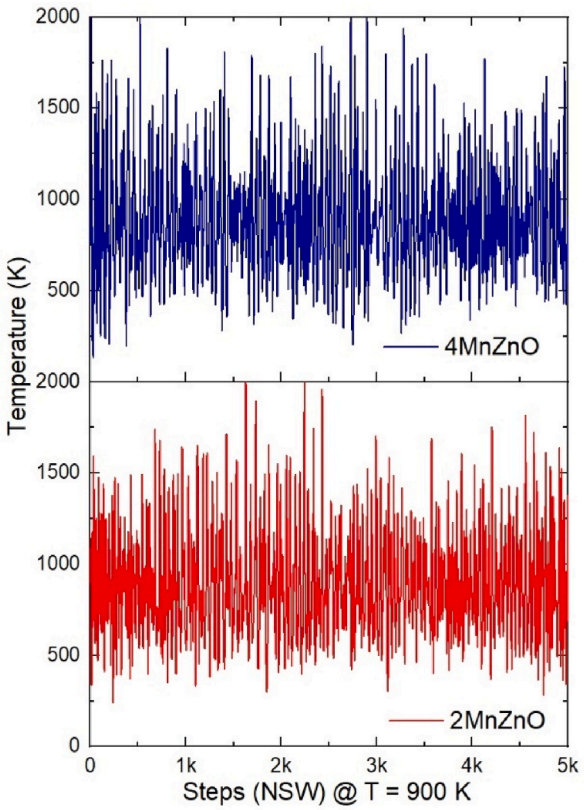

Fig. 11. Temperature profile of 2Mn & 4Mn doped ZnO system.

can be termed as thermally stable.

4. Conclusion

Adopting first-principles density functional theory, band structures, optical properties, elastic constants and atomic structure of pure ZnO and doped ZnO system have been studied and analyzed in a detailed manner. Two different doping levels have been employed by addition of 2 Manganese atoms and 4 Manganese atoms in the pure ZnO system and the changes in behavior of system have been investigated. The presence of manganese atoms in the system greatly modified the band structures of pure ZnO system. Band structures obtained for the pure and doped ZnO system indicate that the energy gap has been reduced and DOS indicate that the greater concentration of electrons occur near conduction band. Analysis of optical parameters reveals that the static reflectivity and refractive index has increased considerably after addition of Mn atom in the ZnO system. While some minor changes are recorded at higher energy ranges. Similarly, absorption coefficient of ZnO system has improved greatly at lower energy ranges and new peaks are emerged. It is worth noticing that the new peaks are at lower ranges, which is evidence of red shift. The shift is towards the visible range of optical spectrum and suggests that the material can be used for piezoelectric and solar applications. The computed elastic constants predicts that the modification has retained the stability and can be used for various applications. Also the XRD Spectra depicts that the geometry has accepted the dopants and no new peaks are observed in comparative analysis. The phonon dispersion calculation reveal that the Manganese can be used as a dopant for performance improvement of ZnO due to its dynamic stability. Also the temperature profile predicts Manganese as thermally stable to be used as dopant in ZnO system.

The outcome of this study serves a basis for use of transition metal as dopant in the ZnO system which can used for various applications like piezoelectric and solar, a step towards smart energy development.

Data availability

Data will be made available on request.

CRediT authorship contribution statement

Rasool Akhtar Alias Osama: Writing – review & editing, Writing – original draft, Validation, Project administration, Methodology, Investigation, Formal analysis, Data curation, Conceptualization. **Sadia Abdul Samad:** Writing – review & editing, Validation, Software, Methodology, Investigation, Formal analysis, Conceptualization. **Samia Saher:** Validation, Software, Methodology, Investigation. **Muhammad Rafique:** Writing – review & editing, Supervision, Project administration. **Rebecca Cheung:** Writing – review & editing, Supervision, Project administration.

Declaration of competing interest

The authors declare that they have no known competing financial interests or personal relationships that could have appeared to influence the work reported in this paper.

Acknowledgements

This work was supported by the University of Edinburgh, the CASTEP Developers' Group (CDG), Cambridge Enterprise and Higher Education Commission of Pakistan.

References

[1] S. Singh, et al., Structure, microstructure and physical properties of ZnO based materials in various forms: bulk, thin film and nano, J. Phys. Appl. Phys. 40 (20) (2007) 6312–6327.
[2] B. Abebe, et al., A review on enhancing the antibacterial activity of ZnO: mechanisms and microscopic investigation, Nanoscale Res. Lett. 15 (1) (2020) 190.
[3] M.-P. Lu, M.-Y. Lu, L.-J. Chen, p-Type ZnO nanowires: from synthesis to nanoenergy, Nano Energy 1 (2) (2012) 247–258.
[4] D. Tan, Y. Xiang, Y.S. Leng, Molecular simulation study of piezoelectric potential distribution in a ZnO nanowire under mechanical bending, Mrs Advances 2 (56) (2017) 3433–3439.
[5] H.-C. Wu, Y.-C. Peng, C.-C. Chen, Effects of Ga concentration on electronic and optical properties of Ga-doped ZnO from first principles calculations, Opt. Mater. 35 (3) (2013) 509–515.
[6] L. Serairi, Y. Leprince-Wang, ZnO nanowire-based piezoelectric nanogenerator device performance tests, Crystals 12 (8) (2022).
[7] R. Tao, et al., Flexible piezoelectric transducers based on a Pmma/Zno nanowire composite. 2017 Joint International Eurosoi Workshop and International Conference on Ultimate Integration on Silicon (Eurosoi-Ulis 2017), 2017, pp. 188–191.
[8] J.H. Song, et al., Piezoelectric potential output from ZnO nanowire functionalized with p-type oligomer, Nano Lett. 8 (1) (2008) 203–207.
[9] H.-C. Wu, Y.-C. Peng, T.-P. Shen, Electronic and optical properties of substitutional and interstitial Si-doped ZnO, Materials 5 (11) (2012) 2088–2100.
[10] S. Rackauskas, et al., ZnO nanowire application in chemoresistive sensing: a review, Nanomaterials 7 (11) (2017).
[11] R.A. Qadr, D.R. Saber, S.B. Aziz, Theoretical investigations of electronic and optical properties of vanadium doped wurtzite Zinc Oxide from first principle calculation method, Iraqi Journal of Physics (IJP) 20 (2) (2022) 38–52.
[12] M.Z. Rahaman, H. Tanaka, A.K.M. Akther Hossain, An experimental and theoretical insights into the dielectric properties of (Li, Nd) co-doped ZnO ceramics, J. Mater. Sci. Mater. Electron. 31 (22) (2020) 20113–20128.
[13] H. Saadi, et al., Effect of Co doping on the physical properties and organic pollutant photodegradation efficiency of ZnO nanoparticles for environmental applications, Nanomaterials 14 (1) (2024).

[14] H. Saadi, et al., Enhancing the electrical conductivity and the dielectric features of ZnO nanoparticles through Co doping effect for energy storage applications, J. Mater. Sci. Mater. Electron. 34 (2) (2023).
[15] Y.P. Mao, et al., Self-powered wearable athletics monitoring nanodevice based on ZnO nanowire piezoelectric-biosensing unit arrays, Sci. Adv. Mater. 11 (3) (2019) 351–359.
[16] M. Ramzan, et al., Optimization of electronic and optical properties of transition metal doped ZnO by DFT+U method and supported by experimental findings, Mater. Today Commun. 33 (2022).
[17] G. Tse, The optical and elastic properties of strained ZnO by first principle calculations, Computational Condensed Matter 26 (2021).
[18] Q. Hou, et al., First principles study of carrier activity, lifetime and absorption spectrum to investigate effects of strain on the photocatalytic performance of doped ZnO, Curr. Appl. Phys. 33 (2022) 41–50.
[19] B. Ul Haq, et al., Investigations of optoelectronic properties of novel ZnO monolayers: a first-principles study, Mater. Sci. Eng., B (2021) 265.
[20] H. Soleimani, CASTEP study on electronic and optical properties of Zinc oxid, Recent Advances in Petrochemical Science 1 (3) (2017).
[21] X. Zhang, et al., Characterizing and optimizing piezoelectric response of ZnO nanowire/PMMA composite-based sensor, Nanomaterials 11 (7) (2021).
[22] O. Sublemontier, et al., X-Ray photoelectron spectroscopy of isolated nanoparticles, J. Phys. Chem. Lett. 5 (19) (2014) 3399–3403.
[23] L. Kang, et al., La-doped p-type ZnO nanowire with enhanced piezoelectric performance for flexible nanogenerators, Appl. Surf. Sci. 475 (2019) 969–973.
[24] Z.Y. Gao, et al., Effects of piezoelectric potential on the transport characteristics of metal-ZnO nanowire-metal field effect transistor, J. Appl. Phys. 105 (11) (2009).
[25] C. Opoku, et al., Fabrication of ZnO nanowire based piezoelectric generators and related structures, Proceedings of the 2015 ICU International Congress on Ultrasonics 70 (2015) 858–862.
[26] R. Amari, et al., Effects of Mn doping on the structural, morphological, electronic and optical properties of ZnO thin films by sol-gel spin coating method: an experimental and DFT+U study, Phys. B Condens. Matter 577 (2020).
[27] E. Ozugurlu, Cd-doped ZnO nanoparticles: an experimental and first-principles DFT studies, J. Alloys Compd. (2021) 861.
[28] X.X. Zhang, et al., Self-powered ethanol gas sensor based on the piezoelectric Ag/ZnO nanowire arrays at room temperature, J. Mater. Sci. Mater. Electron. 32 (6) (2021) 7739–7750.
[29] L. Wang, et al., Improved piezoresistive properties of ZnO/SiC nanowire heterojunctions with an optimized piezoelectric nanolayer, J. Mater. Sci. 56 (30) (2021) 17146–17155.
[30] H. Tong, B.L. Wang, Z.C. Ou-Yang, Electric potential generated in ZnO nanowire due to piezoelectric effect, Thin Solid Films 516 (9) (2008) 2708–2710.
[31] M. Riaz, et al., Study of the piezoelectric power generation of ZnO nanowire arrays grown by different methods, Adv. Funct. Mater. 21 (4) (2011) 628–633.
[32] G. Poulin-Vittrant, et al., Fabrication and characterization of ZnO nanowire-based piezoelectric nanogenerators for low frequency mechanical energy harvesting, Proceedings of the 2015 Icu International Congress on Ultrasonics 70 (2015) 909–913.
[33] M.P. Lu, et al., Piezoelectric nanogenerator using p-type ZnO nanowire arrays, Nano Lett. 9 (3) (2009) 1223–1227.
[34] S.S. Kwon, et al., Piezoelectric effect on the electronic transport characteristics of ZnO nanowire field-effect transistors on bent flexible substrates, Adv. Mater. 20 (23) (2008) 4557–4562.
[35] C. Justeau, et al., A comparative study on the effects of Au, ZnO and AZO seed layers on the performance of ZnO nanowire-based piezoelectric nanogenerators, Materials 12 (16) (2019).
[36] S.B. Joe, S.M. Shaby, Characterization and performance analysis of piezoelectric ZnO nanowire for low-frequency energy harvesting applications, Appl. Nanosci. (2021).
[37] I.Y.Y. Bu, Paper-based, sound driven piezoelectric ZnO nanowire devices, Solid State Electron. 130 (2017) 1–3.
[38] R. Muhammad, Y. Shuai, H.-P. Tan, A first-principles study on alkaline earth metal atom substituted monolayer boron nitride (BN), J. Mater. Chem. C 5 (32) (2017) 8112–8127.
[39] M. Rafique, et al., Manipulating intrinsic behaviors of graphene by substituting alkaline earth metal atoms in its structure, RSC Adv. 7 (27) (2017) 16360–16370.
[40] M. Rafique, Y. Shuai, N. Hussain, First-principles study on silicon atom doped monolayer graphene, Phys. E Low-dimens. Syst. Nanostruct. 95 (2018) 94–101.
[41] R. Muhammad, Y. Shuai, H.-P. Tan, First-principles study on hydrogen adsorption on nitrogen doped graphene, Phys. E Low-dimens. Syst. Nanostruct. 88 (2017) 115–124.
[42] M. Rafique, Y. Shuai, M. Hassan, Structural, electronic and optical properties of CO adsorbed on the defective anatase TiO 2 (101) surface; a DFT study, J. Mol. Struct. 1142 (2017) 11–17.
[43] C.-Y. Tu, J.M. Wu, Localized surface plasmon resonance coupling with piezophototronic effect for enhancing hydrogen evolution reaction with Au@MoS2 nanoflowers, Nano Energy 87 (2021).
[44] R. Muhammad, Y. Shuai, T. He-Ping, First-principles Study of Electronic and Optical Properties of Boron and Nitrogen Doped Graphene, 2017.
[45] J. Okabayashi, et al., Detecting quadrupole: a hidden source of magnetic anisotropy for Manganese alloys, Sci. Rep. 10 (1) (2020) 9744.
[46] S. Koseki, et al., Spin-orbit coupling constants in atoms and ions of transition elements: comparison of effective core potentials, model core potentials, and all-electron methods, J. Phys. Chem. A 123 (12) (2019) 2325–2339.
[47] Z.Y. Gao, et al., Effects of piezoelectric potential on the transport characteristics of metal-ZnO nanowire-metal field effect transistor, 105, 113707, 2009), J. Appl. Phys. 106 (3) (2009).
[48] T. Groń, et al., Spin-orbit coupling in manganese doped calcium molybdato-tungstates, Ceram. Int. 44 (3) (2018) 3307–3313.
[49] C. Fisk, C. Valdemoro, S. Fraga, Spin–orbit coupling in some positive ions of Cr, Mn, and Fe, J. Chem. Phys. 48 (7) (1968) 2923–2925.
[50] T. Dahame, et al., Electronic structure, first and second order physical properties of MPS4: a theoretical study, Materials Science-Poland 34 (2) (2016) 275–285.
[51] M. Sartorato, R. de Medeiros, V. Tita, A finite element formulation for smart piezoelectric composite shells: mathematical formulation, computational analysis and experimental evaluation, Compos. Struct. 127 (2015) 185–198.